

# Response of Holographic QCD to Electric and Magnetic Fields

---

**Oren Bergman\***

*School of Natural Sciences  
Institute for Advanced Study  
Princeton, NJ 08540, USA*  
[bergman@sns.ias.edu](mailto:bergman@sns.ias.edu), [bergman@physics.technion.ac.il](mailto:bergman@physics.technion.ac.il)

**Gilad Lifschytz**

*Department of Mathematics and Physics and CCMSC  
University of Haifa at Oranim  
Tivon 36006, Israel*  
[giladl@research.haifa.ac.il](mailto:giladl@research.haifa.ac.il)

**Matthew Lippert**

*Department of Physics  
Technion, Haifa 32000, Israel*  
and  
*Department of Mathematics and Physics  
University of Haifa at Oranim  
Tivon 36006, Israel*  
[matthewslippert@gmail.com](mailto:matthewslippert@gmail.com)

**ABSTRACT:** We study the response of the Sakai-Sugimoto holographic model of large  $N_c$  QCD at nonzero temperature to external electric and magnetic fields. In the electric case we find a first-order insulator-conductor transition in both the confining and deconfining phases of the model. In the deconfining phase the conductor is described by the parallel 8-brane-anti-8-brane embedding with a current of quarks and anti-quarks. We compute the conductivity and show that it agrees precisely with a computation using the Kubo formula. In the confining phase we propose a new kind of 8-brane embedding, corresponding to a baryonic conductor. In the magnetic field case we show that the critical temperature for chiral-symmetry restoration in the deconfined phase increases with the field and approaches a finite value in the limit of an infinite magnetic field. We also illustrate the nonlinear behavior of the electric and magnetic susceptibilities in the different phases.

---

\*On sabbatical leave from the Department of Physics, Technion, Haifa 32000, Israel.

---

## Contents

<b>1. Introduction and Summary</b>	<b>1</b>
<b>2. Review of the Sakai-Sugimoto model</b>	<b>2</b>
<b>3. Electric Field</b>	<b>5</b>
3.1 Deconfined phase	6
3.1.1 Conductivity at finite density	9
3.2 Conductivity and the Kubo formula	9
3.3 Confined phase	10
3.4 Electric susceptibility	13
<b>4. Magnetic field</b>	<b>14</b>
4.1 Deconfined phase	14
4.2 Confined phase	15
4.3 Magnetic susceptibility	16

---

## 1. Introduction and Summary

Holographic descriptions of large  $N_c$  QCD-like theories have received a great deal of attention recently (for a recent review see [1]). The models involve the physics of  $N_f$  flavor-brane probes in near-horizon geometries of  $N_c$  color-branes. The Sakai-Sugimoto D4-D8- $\overline{D8}$  model [2] in particular is very attractive in that it has a simple geometric description of chiral symmetry breaking, and appears to be rich enough to incorporate, at least qualitatively, all the low energy features of QCD. The properties of the mesons [2, 3] and baryons [4], the resolution of the  $U(1)_A$  problem [5], and the phase diagram at nonzero temperature [6, 7], nonzero baryon chemical potential [8, 9], and nonzero isospin chemical potential [10], all exhibit many similarities with QCD. While the original model had only massless quarks, it can be generalized to nonzero quark mass [11].

The Sakai-Sugimoto model does not include a true electromagnetic gauge field, but we can mimic the effect of one using the Abelian part of the flavor symmetry. In this paper we will analyze the Sakai-Sugimoto model at finite temperature with an Abelian background gauge field in the diagonal  $U(1)_V$  part of the D8- $\overline{D8}$  gauge group. This gauge field is holographically dual to the baryon number current of the four-dimensional gauge theory. Except for the one-flavor case, this is not the same as an electromagnetic field, since “up” and “down” type quarks have the same charge. Nevertheless, we expect the physics to be qualitatively similar

to that of a background electromagnetic field. Background flavor gauge fields have been studied previously in the  $\mathcal{N} = 2$  supersymmetric theory corresponding to 7-brane probes in the 3-brane background [12, 13, 14].

We would like to determine the effect of the electric and magnetic fields on the phase diagram of the theory and compute the response coefficients (susceptibilities or conductivities) of the different phases. We will do this by analyzing the 8-brane embeddings in the presence of the appropriate background world-volume gauge field. The value of the 8-brane action is identified in the usual way with the appropriate thermodynamic potential.

In the case of an electric field we find an insulator-conductor type transition, which in the deconfined phase generalizes the chiral symmetry breaking-restoration transition at zero field. The critical temperature decreases with the field. Since we use the DBI action, there is a temperature-dependent maximal value of the electric field. However, the transition to the conductor occurs at a smaller value of the field. We compute the conductivity in the conducting phase and show that it agrees precisely, in the zero field limit, with what is expected from the Kubo formula. This agreement extends to the nonzero density case as well. Somewhat surprisingly, we also find an insulator-conductor transition in the confined phase, where there is no chiral-symmetric phase. We propose that the conducting phase corresponds to an embedding in which the 8-brane and anti-8-brane are geodesically parallel and connect at a cusp at the “tip of the cigar”. We compute the conductivity of this embedding and determine the phase diagram. The current in this case is carried by baryons and anti-baryons.

With a magnetic field we observe that the critical temperature for chiral symmetry restoration increases with the field, in agreement with expectations for QCD. We find that the critical temperature approaches a finite value in the limit of infinite field, which differs from the behavior in the  $\mathcal{N} = 2$  theory found in [13, 14].

The paper is organized as follows: In section 2 we review briefly the Sakai-Sugimoto model and set up our conventions; sections 3 and 4 deal with, respectively, the physics of background electric and magnetic fields.

## 2. Review of the Sakai-Sugimoto model

The model consists of  $N_c$  D4-branes in Type IIA string theory wrapping a circle with anti-periodic boundary conditions for fermions,  $N_f$  D8-branes at a point on the circle, and  $N_f$  anti-D8-branes at another point on the circle. At energies well below the Kaluza-Klein scale the spectrum on the D4-branes is precisely that of massless four-dimensional “QCD”, with  $N_c$  colors of gluons and  $N_f$  flavors of quarks. The holographic dual description comes about by taking the large  $N_c$  limit, in which the D4-branes are replaced by their near-horizon supergravity background. It is most convenient to work in units in which the curvature radius is fixed to unity,  $R = (\pi g_s N_c)^{1/3} \sqrt{\alpha'} = 1$ . Taking  $x_4$  as the circle direction,  $x_4 \sim x_4 + 2\pi R_4$ ,

the background is given by

$$\begin{aligned}
ds^2 &= u^{\frac{3}{2}} \left( -dx_0^2 + d\mathbf{x}^2 + f(u)dx_4^2 \right) + u^{-\frac{3}{2}} \left( \frac{du^2}{f(u)} + u^2 d\Omega_4^2 \right) \\
e^\Phi &= g_s u^{3/4}, \quad F_4 = 3\pi(\alpha')^{3/2} N_c d\Omega_4,
\end{aligned} \tag{2.1}$$

where  $f(u) = 1 - (u_{KK}^3/u^3)$ , and  $u_{KK} = 4/(9R_4^2)$ . The  $(u, x_4)$  subspace is topologically a cigar (or disk), with a tip at  $u = u_{KK}$ . In the dual gauge theory this ultimately implies that the gluons are confined. The gravitational description is valid as long as  $\lambda \gg R_4$ , where  $\lambda$  is the five-dimensional 't Hooft coupling, which in our units is given by

$$\lambda = 4\pi g_s N_c \sqrt{\alpha'} = \frac{4}{\alpha'}. \tag{2.2}$$

The 8-branes and anti-8-branes are treated as probes in this background, and their embedding determines the flavor physics in the dual gauge theory. Due to the topology of the background the 8-branes and anti-8-branes must connect into a smooth U-shaped configuration at some radial position  $u_0 \geq u_{KK}$  (fig. 1a). This reflects the spontaneous breaking of the  $U(N_f)_R \times U(N_f)_L$  chiral symmetry to the diagonal  $U(N_f)_V$ . The form of the embedding can be determined from the DBI action of the 8-branes in this background,

$$S = \mathcal{N} \int d^4x \int du u^4 \left[ f(u)(x_4'(u))^2 + \frac{1}{u^3 f(u)} \right]^{1/2}. \tag{2.3}$$

The normalization constant is given by

$$\mathcal{N} = 2N_f V_4 \Omega_4 T_8 = \frac{4N_f V_4}{3(2\pi)^6 (\alpha')^{9/2} g_s}, \tag{2.4}$$

where  $V_4$  is the volume of 4d spacetime,  $\Omega_4$  is the volume of a unit 4-sphere, and  $T_8$  is the 8-brane tension. The factor of 2 corresponds to the two halves of the embedding (8-branes and anti-8-branes) along  $u$ . The equation of motion for the embedding  $x_4(u)$  gives

$$x_4'(u) = \frac{1}{u^{3/2} f(u)} \left[ \frac{u^8 f(u)}{u_0^8 f(u_0)} - 1 \right]^{-1/2}. \tag{2.5}$$

Therefore at large  $u$

$$x_4(u) \approx \frac{L}{2} - \frac{2}{9} \frac{c}{u^{9/2}}, \tag{2.6}$$

where  $L$  is the asymptotic 8-brane-anti-8-brane separation,

$$L = 2 \int_{u_0}^{\infty} du x_4'(u), \tag{2.7}$$

and  $c$  is the constant of the motion associated with  $x_4(u)$ . This constant corresponds to the curvature of the 8-brane, and is related to  $u_0$  by

$$c = u_0^4 \sqrt{f(u_0)}. \tag{2.8}$$

At nonzero temperature there are two possible backgrounds. For  $T < 1/(2\pi R_4)$  the dominant background is the Euclidean continuation of (2.1) with  $x_0^E \sim x_0^E + 1/T$ . In this background the 8-brane embedding is the same as above. The glue sector is therefore confined, and chiral symmetry is broken. For  $T > 1/(2\pi R_4)$  the dominant background is given by (2.1), with the roles of  $x_4$  and  $x_0^E$  exchanged and with  $f(u) = 1 - (u_T^3/u^3)$ , where  $u_T = (4\pi T/3)^2$ . Here the  $(u, x_4)$  subspace is topologically a cylinder, with a horizon at  $u = u_T$ , which in the dual gauge theory implies deconfinement. In this background there are two possible 8-brane embeddings: a U-shaped embedding (fig. 1b), that satisfies

$$x_4'(u) = \frac{1}{u^{3/2}\sqrt{f(u)}} \left[ \frac{u^8 f(u)}{u_0^8 f(u_0)} - 1 \right]^{-1/2}, \quad (2.9)$$

and a parallel 8-brane-anti-8-brane embedding with  $x_4'(u) = 0$  (fig. 1c). For  $T < 0.154/L$  the U embedding dominates and therefore chiral symmetry is broken, but when  $T > 0.154/L$  the parallel embedding dominates and chiral symmetry is restored. The intermediate phase of deconfinement and chiral symmetry breaking appears only when this critical temperature is higher than the deconfinement temperature  $1/(2\pi R_4)$ , namely when  $L < 0.97R_4$ . Both the confinement/deconfinement and chiral symmetry breaking/restoration transitions are first order.

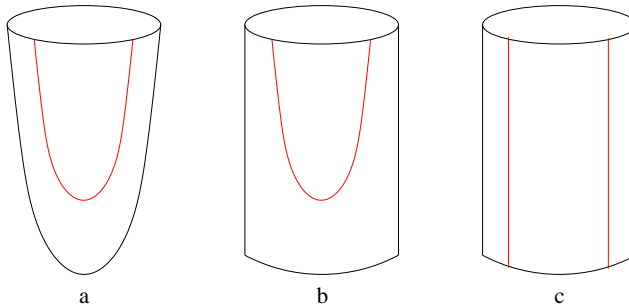


**Figure 1: 8-brane embeddings and phases of the Sakai-Sugimoto model: (a) confined, broken chiral symmetry (b) deconfined, broken chiral symmetry (c) deconfined, restored chiral symmetry**

The 8-brane curvature  $c$  is an order parameter for the chiral symmetry transition in the deconfined phase: it vanishes in the chiral-symmetric parallel embedding, and is given by (2.8) in the chiral symmetry breaking U embedding.<sup>1</sup> By studying the dependence of  $L$  on  $c$  one finds a turn-around behavior typical of a first order phase transition. This is easily seen from the asymptotic behavior of  $L$  at small and large  $c$  (see fig. 2 for a numerical plot of  $L$

<sup>1</sup>This is not the usual chiral symmetry order parameter. The 8-brane curvature  $c$  is related to the expectation value of a quark quadra-linear operator [15]. The usual chiral symmetry order parameter is the quark bi-linear  $\langle \bar{q}q \rangle$ , which is given by the normalizable mode of the flavor bi-fundamental scalar field [11].

vs.  $c$  at a fixed temperature, and also [7]),

$$\begin{aligned} c \rightarrow 0 \quad (u_0 \rightarrow u_T) &: L(c, T) \sim c/T^9 \\ c \rightarrow \infty \quad (u_0 \rightarrow \infty) &: L(c, T) \sim c^{-1/8}. \end{aligned} \tag{2.10}$$

This implies that there is a maximal value of the asymptotic separation  $L_{max}$ , which depends on  $T$ . For  $L < L_{max}$  there are actually two U embedding solutions, and for  $L > L_{max}$  there are none. Alternatively, since  $L$  is a monotonically decreasing function of the temperature, there is a maximal temperature  $T_{max}$  at any fixed  $L$ . For  $T < T_{max}$  there are three solutions in all: the parallel embedding, and the two U embeddings. Evidently, one of the U embeddings must be an unstable solution. At  $T = T_{max}$  the unstable U embedding merges with the stable one, and at higher temperatures the two disappear, leaving only the parallel embedding. The transition from the stable U embedding to the parallel embedding occurs at a temperature lower than  $T_{max}$ .

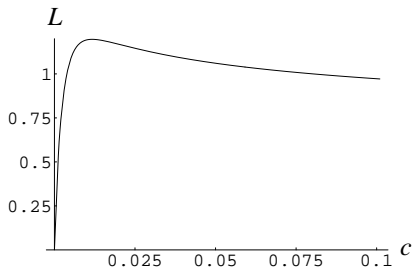


Figure 2:  $L$  vs.  $c$  for the U embedding in the deconfined phase ( $T = 0.14$ )

### 3. Electric Field

In this section we will study the response of the model to an external electric field  $E$ , by turning on an appropriate background value for the Abelian gauge field component of the unbroken  $U(N_f)_V$  gauge field in the 8-brane worldvolume. We normalize this field as follows

$$\hat{A} = \frac{1}{N_f} \text{Tr } \mathcal{A}, \tag{3.1}$$

where  $\mathcal{A}$  is the  $U(N_f)_V$  gauge field.<sup>2</sup> Anticipating a current in the direction of the background field, we make the ansatz (in Euclidean space)

$$\hat{A}_1(x_0, u) = -iEx_0^E + F(u), \tag{3.2}$$

where the  $u$  dependence encodes the current in the usual holographic fashion [12].

---

<sup>2</sup>The canonical normalization is  $\hat{A} = \sqrt{2/N_f} \text{Tr } \mathcal{A}$ , but then the quarks carry  $1/\sqrt{2N_f}$  units of charge. In our normalization the kinetic term has an extra factor of  $2N_f$ , but the quarks carry unit charge. This normalization is more suitable to mimic an electromagnetic field.

### 3.1 Deconfined phase

We begin in the deconfining background, which dominates when  $T > 1/(2\pi R_4)$ . The DBI action for the 8-branes with the gauge field in (3.2) is given by

$$S = \mathcal{N} \int du u^4 \sqrt{\left(f(u)(x'_4)^2 + \frac{1}{u^3}\right) \left(1 - \frac{e^2}{f(u)u^3}\right) + \frac{f(u)(a'_1)^2}{u^3}}, \quad (3.3)$$

where we have defined the dimensionless quantities  $a_1 \equiv 2\pi\alpha'\hat{A}_1$  and  $e \equiv 2\pi\alpha'E$ . The asymptotic behavior of the gauge field is given by

$$a_1(x_0, u) \sim -ie x_0^E - \frac{2}{3} \frac{j}{u^{3/2}}, \quad (3.4)$$

where  $j$  is the conserved charge associated with  $a_1$ , namely the baryon number current. The physical dimensionful current is given in our units by  $J = (2\pi\alpha'\mathcal{N}/V_4)j$ . In terms of the current the action becomes

$$S = \mathcal{N} \int du u^4 \sqrt{\left(f(u)x_4'^2 + \frac{1}{u^3}\right) \left(f(u) - \frac{e^2}{u^3}\right) \left(f(u) - \frac{j^2}{u^5}\right)^{-1}}. \quad (3.5)$$

This form of the action displays a generalization of the usual limiting electric field of the flat space DBI action. For a vanishing current, the action is complex, and the embedding is unphysical, if the second factor becomes negative anywhere in the integration region. However this can be fixed by turning on a current such that the third factor changes sign at the same point. This gives an equation relating the current and the electric field [12].

As in the zero field case there are two types of embedding. Consider first a U embedding with a vanishing current,  $j = 0$ . The solution satisfies

$$x'_4(u) = \frac{1}{u^{3/2}\sqrt{f(u)}} \left[ \frac{u^8 \left(f(u) - \frac{e^2}{u^3}\right)}{u_0^8 \left(f(u_0) - \frac{e^2}{u_0^3}\right)} - 1 \right]^{-1/2}, \quad (3.6)$$

and the large  $u$  behavior is given by (2.6), with

$$c = u_0^4 \sqrt{f(u_0) - \frac{e^2}{u_0^3}}. \quad (3.7)$$

The action of this solution is given by

$$S^U = \mathcal{N} \int_{u_0}^{\infty} du u^{5/2} \sqrt{1 - \frac{e^2}{u^3 f(u)}} \left[ 1 - \frac{u_0^8 \left(f(u_0) - \frac{e^2}{u_0^3}\right)}{u^8 \left(f(u) - \frac{e^2}{u^3}\right)} \right]^{-1/2}. \quad (3.8)$$

The U embedding with  $j = 0$  is always physical: since  $c$  is real, the solution satisfies  $e^2 \leq u_0^3 f(u_0)$ , and the action is real. A current may be turned on, as long as  $j^2 < u_0^5 f(u_0)$ , but

this increases the action, so the dominant U embedding has  $j = 0$ . In the gauge theory this embedding therefore corresponds to a chiral-symmetry breaking, insulating phase.

In fact the U embedding satisfies an even tighter bound on the electric field than above. As in the zero field case, at fixed values of  $e$  and  $T$ , there is a maximal value of  $L$  as a function of  $c$  for the U embedding. Since  $L$  is a monotonically decreasing function of  $e$ , this implies a maximal value of  $e$  as a function of  $c$  at fixed values of  $L$  and  $T$ . The maximal value  $e_{max}$  is attained at some  $c > 0$ , which, using (3.7), implies that  $e_{max}^2 < u_0^3 f(u_0)$ . For  $e > e_{max}$  there are no U embedding solutions, and we therefore expect a phase transition to occur, at fixed  $T$  and  $L$ , at some value of  $e$  smaller than  $e_{max}$ .

In the parallel embedding  $x'_4(u) = 0$ , and the action is given by

$$S^{\parallel} = \mathcal{N} \int_{u_T}^{\infty} du u^{5/2} \sqrt{\frac{f(u) - \frac{e^2}{u^3}}{f(u) - \frac{j^2}{u^5}}}. \quad (3.9)$$

The numerator is negative for  $u^3 < e^2 + u_T^3$ , which is always in the range of integration. The only way to ensure a real action in this case is for the denominator to become negative at the same  $u$ . This requires a nonzero current given by

$$j = e(e^2 + u_T^3)^{1/3}. \quad (3.10)$$

The parallel embedding therefore describes a chiral-symmetric conducting phase in the gauge theory, and the conductivity is given by

$$\sigma = \frac{J}{E} = \frac{(2\pi\alpha')^2 \mathcal{N}}{V_4} (e^2 + u_T^3)^{1/3} = \frac{N_f N_c \lambda T^2}{27\pi} (1 + \tilde{e}^2)^{1/3}, \quad (3.11)$$

where we have defined a new dimensionless variable  $\tilde{e}$  by

$$\tilde{e} \equiv \frac{e}{u_T^{3/2}} = \frac{27}{8\pi^2} \frac{E}{\lambda T^3}. \quad (3.12)$$

To determine which phase dominates as a function of the temperature and electric field we should in principle compare the electric free energies of the two solutions, which are in turn defined by the Euclidean 8-brane action of the solutions

$$\mathcal{F}_e(L, e, T) = TS[x_4(u), a_1(u), T]_{EOM}. \quad (3.13)$$

However this is not quite right for the parallel embedding. First of all, the conducting phase is not in equilibrium. There is a steady state current with a finite conductivity, meaning that energy must be constantly added to the system. This energy is dissipated into the gluon “bath”, which, in general, raises the temperature. At large  $N_c$ , however, this effect is negligible. While the dissipated energy is  $\mathcal{O}(N_c)$ , there are  $\mathcal{O}(N_c^2)$  gluons among which to distribute this energy, so the temperature rise is only  $\mathcal{O}(N_c^{-1})$ . But even ignoring the dissipation, one still needs to subtract the kinetic energy of the current carriers, which should not be taken as part of the budget at the phase transition.



Alternatively, we can get around this problem using a Maxwell-like construction for the order parameter

$$c = \left. \frac{\partial \mathcal{F}_e}{\partial L} \right|_{e,T}. \quad (3.14)$$

In the parallel embedding  $c = 0$  for any  $L$ . In the U embedding the dependence of  $c$  on  $L$  can be determined numerically using (2.7) and (3.7). Note that here we need the full solution, not just the asymptotic behavior. The result is qualitatively the same as in the zero field case (fig. 2). The transition occurs at the value of  $L$  such that the two bounded areas are equal (see fig. 3 for an illustration). We can then construct the phase diagram in the  $(T, e)$

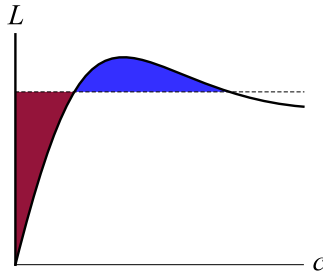


**Figure 3: Illustration of the Maxwell construction**

plane with fixed  $L$  by repeating this procedure for various values of  $e$  and  $T$ , and finding the points which have the same critical  $L$ . The result, shown in fig. 4, shows a first-order insulator-conductor transition at nonzero temperature and background electric field. At zero electric field this reduces to the chiral-symmetry breaking-restoration transition.

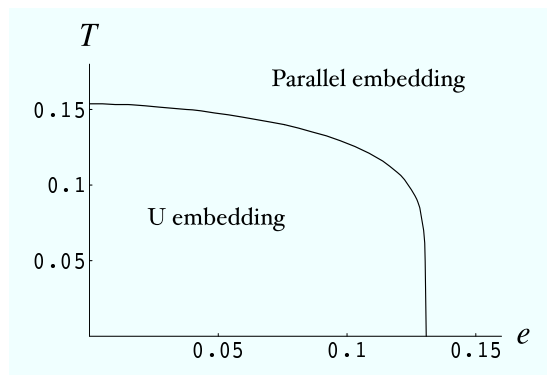


**Figure 4: Phase diagram at nonzero temperature and electric field in the deconfining background ( $L = 1$ )**

### 3.1.1 Conductivity at finite density

The conductivity computed in (3.11) is for the vacuum at a finite temperature. It has two contributions corresponding to quantum and thermal pair-creation of quarks and anti-quarks. The introduction of a finite charge density should also contribute to the conductivity. We can compute this by generalizing our analysis in the parallel embedding to the finite density case. At nonzero density there is a non-trivial time-component of the gauge field  $a_0(u)$ , and the associated constant of the motion is the dimensionless baryon number charge density  $d$ . The dimensionful charge density is  $D = (2\pi\alpha'\mathcal{N}/V_4)d$ . The 8-brane action is<sup>3</sup>

$$S = \mathcal{N} \int du u^4 \sqrt{\left(f(u)(x'_4)^2 + \frac{1}{u^3}\right) \left(1 - \frac{e^2}{f(u)u^3}\right) + \frac{f(u)(a'_1)^2}{u^3} - \frac{(a'_0)^2}{u^3}}. \quad (3.15)$$

In terms of the current and density, the action of the parallel embedding becomes

$$S^{\parallel} = \mathcal{N} \int_{u_T}^{\infty} du u^{5/2} \sqrt{\frac{f(u) - \frac{e^2}{u^3}}{f(u) - \frac{j^2 - f(u)d^2}{u^5}}}. \quad (3.16)$$

The condition for reality now gives

$$j = e \left[ (e^2 + u_T^3)^{2/3} + \frac{d^2}{e^2 + u_T^3} \right]^{1/2}, \quad (3.17)$$

and the conductivity is therefore

$$\begin{aligned} \sigma &= \frac{(2\pi\alpha')^2 \mathcal{N}}{V_4} \left[ (e^2 + u_T^3)^{2/3} + \frac{d^2}{e^2 + u_T^3} \right]^{1/2} \\ &= \frac{N_f N_c \lambda T^2}{27\pi} \left[ (1 + \tilde{e}^2)^{2/3} + \frac{\tilde{d}^2}{1 + \tilde{e}^2} \right]^{1/2}, \end{aligned} \quad (3.18)$$

where we have defined a new dimensionless (with appropriate factors of  $R$ , which in our units is 1) variable  $\tilde{d}$ ,

$$\tilde{d} \equiv \frac{d}{u_T^{5/2}} = \frac{729}{8\pi N_f N_c} \frac{D}{\lambda^2 T^5}. \quad (3.19)$$

At zero charge density this reduces to the vacuum result (3.11).

### 3.2 Conductivity and the Kubo formula

The electrical conductivity is an example of a transport coefficient that describes the response of a thermodynamic system to a disturbance which takes it out of equilibrium. For a small

---

<sup>3</sup>There is also CS term of the form  $\int a_0 a'_1 (\partial_2 a_3 - \partial_3 a_2)$ . However this can be consistently set zero by the equations of motion since  $a_0$  and  $a_1$  are assumed to be independent of  $x_2$  and  $x_3$ .

disturbance, *i.e.* near equilibrium, transport coefficients can be related to real-time correlation functions at equilibrium via Kubo formulas. The electrical conductivity near equilibrium is related to the current-current correlator [16],

$$\sigma = \lim_{k_0 \rightarrow 0} \frac{1}{4T} \text{Tr} C_{\mu\nu}^<(k_0 = |\mathbf{k}|), \quad (3.20)$$

where

$$C_{\mu\nu}^<(k) = \int d^4x e^{-ik \cdot x} \langle J_\mu(0) J_\nu(x) \rangle. \quad (3.21)$$

The correlator can in turn be computed at strong coupling using the Lorentzian AdS/CFT prescription of [17].<sup>4</sup> It is therefore interesting to compare the result of this computation with the direct computation of the conductivity in the previous section. Since the Kubo formula gives the conductivity near equilibrium, one should compare the result with the zero electric field limit of (3.18).

The current-current correlator for light-like momenta has been analyzed in the Sakai-Sugimoto model at both finite temperature and density in [18]. In particular the high-temperature, or equivalently low frequency, behavior was found to be<sup>5</sup>

$$\lim_{k_0 \rightarrow 0} \text{Tr} C^<(k_0 = |\mathbf{k}|) = \frac{2(2N_f)N_c\lambda T^3}{27\pi} \sqrt{1 + \tilde{D}^2}, \quad (3.22)$$

leading to a conductivity

$$\sigma = \frac{N_f N_c \lambda T^2}{27\pi} \sqrt{1 + \tilde{D}^2}, \quad (3.23)$$

in perfect agreement with the zero field limit of (3.18).

### 3.3 Confined phase

For  $T < 1/(2\pi R_4)$  the confining background dominates, and the 8-brane action with the background gauge field is

$$\begin{aligned} S &= \mathcal{N} \int du u^4 \sqrt{\left( f(u)(x'_4)^2 + \frac{1}{f(u)u^3} \right) \left( 1 - \frac{e^2}{u^3} \right) + \frac{(a'_1)^2}{u^3}} \\ &= \mathcal{N} \int du u^4 \sqrt{\left( f(u)x'_4{}^2 + \frac{1}{f(u)u^3} \right) \left( 1 - \frac{e^2}{u^3} \right) \left( 1 - \frac{j^2}{u^5} \right)^{-1}}. \end{aligned} \quad (3.24)$$

At zero field the only possible embedding in the confined phase was the U embedding. However as we increase the electric field we encounter a puzzle. As in the deconfined phase, the U

<sup>4</sup>This prescription actually yields the retarded correlator  $C_{\mu\nu}^R(k) = i \int d^4x e^{-ik \cdot x} \theta(x_0) \langle [J_\mu(0), J_\nu(x)] \rangle$ , which is related to the one above by  $C_{\mu\nu}^<(k) = 2\text{Im} C_{\mu\nu}^R(k)/(e^{-k_0/T} - 1)$ .

<sup>5</sup>Our definition of  $\lambda$  is different than in [18]:  $\lambda_{\text{here}} = 4\pi\lambda_{\text{there}}$ . Our  $\tilde{D}$  is exactly their  $\tilde{C}$ .

embedding solution at a fixed  $L$  ceases to exist above a certain value of the field. To see this we again study the behavior of  $L$  as a function of  $c$ . The U embedding with  $j = 0$  satisfies

$$x'_4(u) = \frac{1}{u^{3/2}f(u)} \left[ \frac{u^8 f(u) \left(1 - \frac{e^2}{u^3}\right)}{u_0^8 f(u_0) \left(1 - \frac{e^2}{u_0^3}\right)} - 1 \right]^{-1/2}, \quad (3.25)$$

and

$$c = u_0^4 \sqrt{f(u_0) \left(1 - \frac{e^2}{u_0^3}\right)}. \quad (3.26)$$

There are two cases to consider. For  $e^2 < u_{KK}^3$ ,  $L(c)$  decreases monotonically from  $L(0) = \pi R_4$  (the anti-podal embedding) to zero as  $c \rightarrow \infty$  (fig. 5a). For  $e^2 > u_{KK}^3$  the asymptotic behavior of  $L(c)$  is the same as in the deconfined phase (fig. 5b), implying a maximal  $L$  for a given  $e$ , or alternatively a maximal  $e$  for a given  $L$ . This maximal value therefore satisfies  $u_{KK}^3 < e_{max}^2 < u_0^3$ . The U embedding exists only for  $e < e_{max}$ , and its action is given by

$$S^U = \mathcal{N} \int_{u_0}^{\infty} du \frac{u^{5/2}}{\sqrt{f(u)}} \sqrt{1 - \frac{e^2}{u^3}} \left[ 1 - \frac{u_0^8 f(u_0) \left(1 - \frac{e^2}{u_0^3}\right)}{u^8 f(u) \left(1 - \frac{e^2}{u^3}\right)} \right]^{-1/2}. \quad (3.27)$$

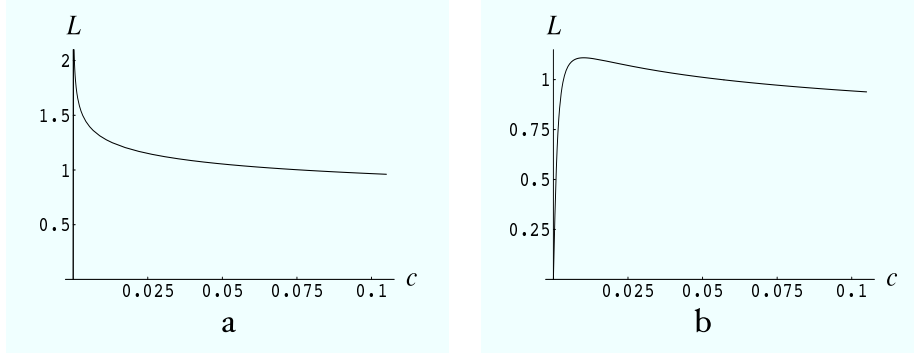


**Figure 5:**  $L$  vs.  $c$  in the confined phase (a)  $e < u_{KK}^{3/2}$  (b)  $e > u_{KK}^{3/2}$

The question is what happens when  $e > e_{max}$ ? There must exist a second embedding that takes over before reaching the maximal electric field. In the deconfined background this was the current-carrying parallel embedding, and we observed a first-order phase transition at  $e < e_{max}$ . We therefore propose a new kind of 8-brane embedding in the confining background, which is analogous to the parallel embedding in the deconfining background. The 8-brane and anti-8-brane follow parallel radial geodesics and connect at  $u = u_{KK}$  (fig. 6). In this “V-shaped” embedding  $x'_4(u) = 0$  (and therefore  $c = 0$ ) except at the tip, where there is a

cusps (unless we are in the anti-podal embedding, which is smooth). Away from  $u_{KK}$  this is clearly a solution. Its action is given by

$$S^V = \mathcal{N} \int_{u_{KK}}^{\infty} du \frac{u^{5/2}}{\sqrt{f(u)}} \sqrt{\frac{1 - \frac{e^2}{u^3}}{1 - \frac{j^2}{u^5}}} . \quad (3.28)$$

It follows from reality of the action that if  $e^2 > u_{KK}^3$  there must be a current given by  $j = e^{5/3}$ . This embedding is therefore a conductor, with a conductivity

$$\sigma = \frac{(2\pi\alpha')^2 \mathcal{N}}{V_4} e^{2/3} = \frac{N_f N_c}{12\pi^{7/3}} \lambda^{1/3} E^{2/3} . \quad (3.29)$$

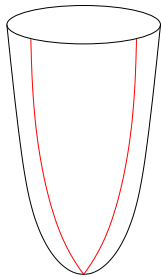


**Figure 6: The conducting V embedding in the confining background**

This proposal raises two questions. The first has to do with stability of the cusp singularity at the tip, and the second with the identification of the current carriers. In the deconfined parallel embedding the current is carried by fundamental strings, namely quarks and anti-quarks. The only charged objects in the confined phase are baryons, so the current can only be carried by baryons and anti-baryons, namely by 4-branes (and anti-4-branes) wrapped on the  $S^4$ . Indeed, this is precisely what we need to source the 5d magnetic field  $a'_1(u)$  dual to the boundary current  $j$ . This is similar to the situation at nonzero density [8], where a uniform distribution of 4-branes was used to source the 5d electric field  $a'_0(u)$  dual to the baryon number density. In that case the 4-branes created a cusp in the 8-brane embedding. In the present case the current corresponds to a uniform distribution of 4-branes and anti-4-branes (since the total charge density vanishes), located at the cusp, and moving at a constant velocity along  $x_1$ . To understand whether this configuration is stable we need to understand the forces at the cusp. In the nonzero density case the upward force due to the 8-brane was balanced against the downward force of the 4-branes. In this case however the 4-branes are at the bottom of the space, and it is not clear how the balance comes about. Higher derivative corrections may also be relevant. We leave this as an open question.

Assuming this is a valid solution, we can construct the phase diagram using the same method as in the deconfined phase. In this case we can either fix  $u_{KK}$  and vary  $L$  and  $e$ , or

fix  $L$  and vary  $u_{KK}$  and  $e$ . The two results are shown in figure 7. From the first diagram we see that for  $e^2 < u_{KK}^3$  the U embedding dominates at all values of  $L$ , and that for  $e^2 \geq u_{KK}^3$  there is a first-order transition to the conducting V embedding at a critical  $L$  that starts at  $\pi R_4$  (the anti-podal embedding) and decreases with  $e$ .

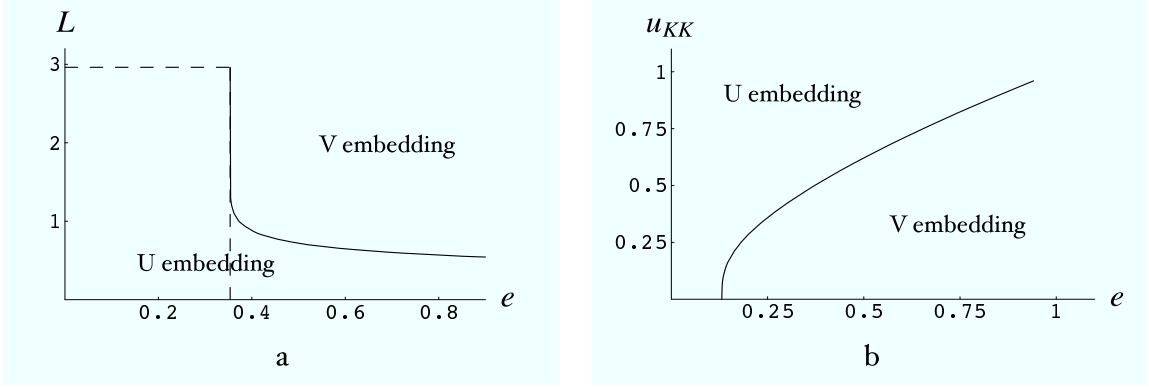


**Figure 7: Electric phase diagram in the confined phase (a) fixed  $u_{KK} = 0.5$  (b) fixed  $L = 1$ . In (a) the dashed lines illustrate that for  $e = u_{KK}^{3/2} \sim 0.35$  the critical  $L = \pi R_4 \sim 3$ .**

The second diagram also provides some interesting insight. First, we note that, for a fixed  $L$ , the critical electric field in the limit  $u_{KK} \rightarrow 0$  in fig. 7b is exactly the same as the critical field in the deconfined phase in the limit  $T \rightarrow 0$  (as seen in fig. 4). This is because both cases are then essentially equivalent to the non-compact model at zero temperature. Second, by comparing the phase diagrams in the confined and deconfined phases at the confinement/deconfinement transition  $u_{KK} = u_T$ , it can be seen that if we start in the confined conducting phase (V embedding) and raise the temperature above the deconfinement temperature we end up in the deconfined conducting phase (parallel embedding). In this transition the conductivity jumps from (3.29) to (3.11).

### 3.4 Electric susceptibility

In both the confined and deconfined phases there is an insulating phase (U embedding) in which the current vanishes. These phases exhibit an electric polarization and susceptibility, which are defined thermodynamically by

$$p = -\frac{\partial \mathcal{F}_e}{\partial e}, \quad \chi_e = -\frac{\partial^2 \mathcal{F}_e}{\partial e^2}. \quad (3.30)$$

In the holographic prescription the free energy is divergent, and requires a counterterm proportional to  $e^2$ . The susceptibility therefore requires a counterterm independent of  $e$ . A physically motivated scheme is to require the susceptibility to vanish at zero field, in other words

$$\chi_e(e) = -\frac{\partial^2 \mathcal{F}_e}{\partial e^2} + \frac{\partial^2 \mathcal{F}_e}{\partial e^2} \Big|_{e=0}. \quad (3.31)$$

This is a measure of the nonlinearity of the vacuum in this model. The results are presented in figure 8.

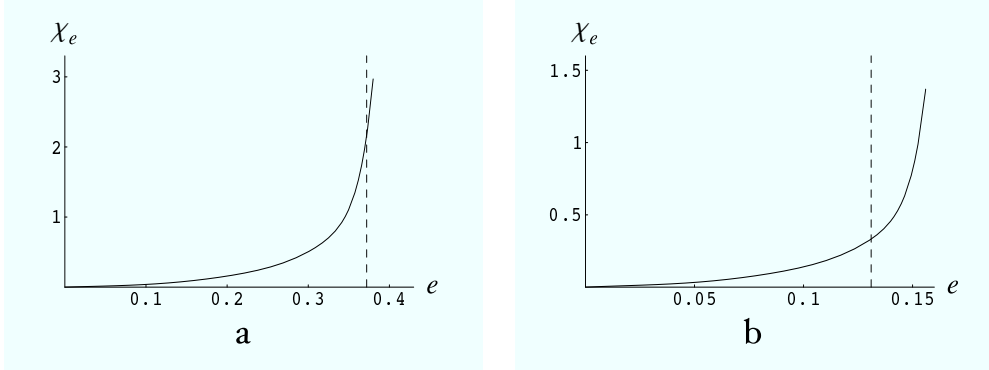


**Figure 8:** Electric susceptibility in the insulating phase of the (a) confined phase, (b) deconfined phase (the dashed line shows the critical field for the insulator/conductor transition).

## 4. Magnetic field

For an external magnetic field  $H$  our ansatz is simply

$$\hat{A}_2(x_1) = Hx_1. \quad (4.1)$$

There will be no current and therefore no  $u$  dependence. Our main objective here is to determine the effect of the background magnetic field on the critical temperature for chiral-symmetry restoration in the deconfined phase. We will also compute the magnetic susceptibility of the vacuum in both the confined and deconfined phases.

### 4.1 Deconfined phase

We start again in the deconfined phase. The 8-brane action in the magnetic field background is given by

$$S = \mathcal{N} \int du u^4 \sqrt{\left(f(u)x_4'^2 + \frac{1}{u^3}\right) \left(1 + \frac{h^2}{u^3}\right)}, \quad (4.2)$$

where  $h \equiv 2\pi\alpha'H$ . The chiral symmetry breaking U embedding now satisfies

$$x_4'(u) = \frac{1}{u^{3/2}\sqrt{f(u)}} \left[ \frac{u^8 \left(f(u) + \frac{h^2}{u^3}\right)}{u_0^8 \left(f(u_0) + \frac{h^2}{u_0^3}\right)} - 1 \right]^{-1/2}, \quad (4.3)$$

and has an action

$$S^U = \mathcal{N} \int_{u_0}^{\infty} du u^{5/2} \sqrt{1 + \frac{h^2}{u^3 f(u)}} \left[ 1 - \frac{u_0^8 \left( f(u_0) + \frac{h^2}{u_0^3} \right)}{u^8 \left( f(u) + \frac{h^2}{u^3} \right)} \right]^{-1/2}. \quad (4.4)$$

In the chiral-symmetric parallel embedding  $x'_4(u) = 0$ , and the action is

$$S^{\parallel} = \mathcal{N} \int_{u_T}^{\infty} du u \sqrt{u^3 + h^2}. \quad (4.5)$$

The actions of the embeddings, which define the magnetic free energies  $\mathcal{F}_m(L, T, h)$ , are divergent, but the difference is finite. The resulting phase diagram (for a fixed value of  $L$ ) is shown in figure 9a. Note that unlike the electric field case, here both embeddings describe equilibrium states, so we can compare the actions directly.

We observe that the temperature at which chiral symmetry is restored increases with the background magnetic field, and approaches a finite value in the limit of an infinite field. This means that above some nonzero temperature chiral symmetry is always restored. A similar increase in the critical temperature for the phase transition in the D3-D7 model was observed in [13, 14], but there is a crucial difference with our result. In the D3-D7 model the critical temperature diverges at a finite value of the magnetic field, which means that there is no phase transition for magnetic fields larger than this value (fig. 9b). It is amusing to speculate whether this can be tested in real QCD, either experimentally or on the lattice.

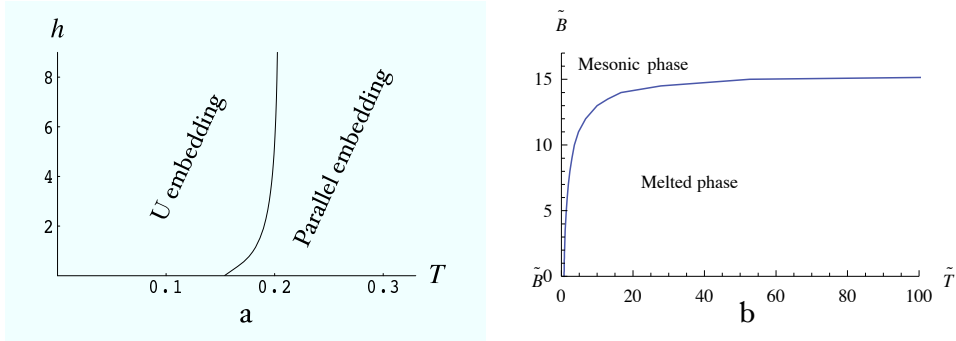


Figure 9: (a) Our phase diagram with a magnetic field (b) analogous phase diagram in the D3-D7 model (reprinted from [14] with the authors' permission).

## 4.2 Confined phase

In the confined phase the 8-brane action is

$$S = \mathcal{N} \int du u^4 \sqrt{\left( f(u) x_4'^2 + \frac{1}{f(u) u^3} \right) \left( 1 + \frac{h^2}{u^3} \right)}. \quad (4.6)$$



The U embedding is basically the same as in the electric case, (3.25) and (3.26), with  $e^2$  replaced by  $-h^2$ . However, the sign difference guarantees that this solution is the only one and that it exists for all values of  $L$  and  $h$ . The action of the solution can also be read off from the electric case (3.27) with the above replacement,

$$S^U = \mathcal{N} \int_{u_0}^{\infty} du \frac{u^{5/2}}{\sqrt{f(u)}} \sqrt{1 + \frac{h^2}{u^3}} \left[ 1 - \frac{u_0^8 f(u_0) \left(1 + \frac{h^2}{u_0^3}\right)}{u^8 f(u) \left(1 + \frac{h^2}{u^3}\right)} \right]^{-1/2}. \quad (4.7)$$

### 4.3 Magnetic susceptibility

The magnetization and magnetic susceptibility are defined thermodynamically by

$$m = -\frac{\partial \mathcal{F}_m}{\partial h}, \quad \chi_m = -\frac{\partial^2 \mathcal{F}_m}{\partial h^2}. \quad (4.8)$$

We can compute the deviation from linearity by regularizing the susceptibility as in the electric case,

$$\chi_m(h) = -\frac{\partial^2 \mathcal{F}_m}{\partial h^2} + \frac{\partial^2 \mathcal{F}_m}{\partial h^2} \Big|_{h=0}. \quad (4.9)$$

The results for all three phases are shown in figure 10.

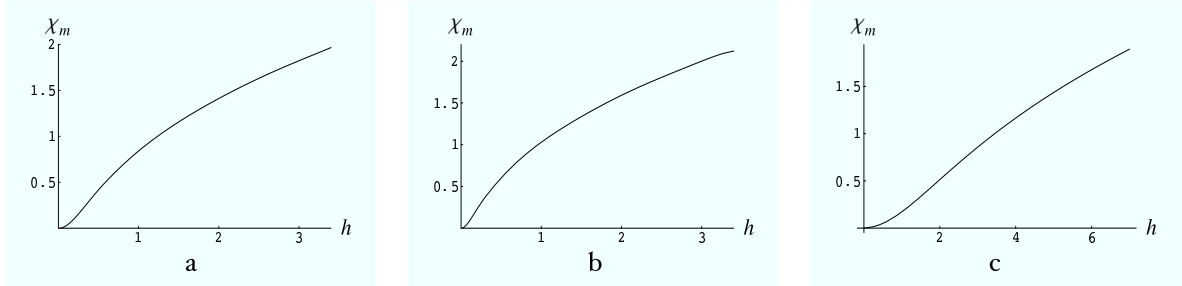


**Figure 10: Magnetic susceptibility: (a) confined, broken chiral symmetry (b) deconfined, broken chiral symmetry (c) deconfined, restored chiral symmetry**

### Acknowledgments

We would like to thank René Meyer and Johanna Erdmenger for useful correspondence. This work was supported in part by the Israel Science Foundation under grant no. 568/05. OB also gratefully acknowledges support from the Institute for Advanced Study.

### References

- [1] J. Erdmenger, N. Evans, I. Kirsch and E. Threlfall, arXiv:0711.4467 [hep-th].

- [2] T. Sakai and S. Sugimoto, *Prog. Theor. Phys.* **113**, 843 (2005) [arXiv:hep-th/0412141]; *Prog. Theor. Phys.* **114**, 1083 (2006) [arXiv:hep-th/0507073].
- [3] K. Peeters, J. Sonnenschein and M. Zamaklar, *JHEP* **0602**, 009 (2006) [arXiv:hep-th/0511044]; F. Bigazzi and A. L. Cotrone, *JHEP* **0611**, 066 (2006) [arXiv:hep-th/0606059]; K. Peeters, J. Sonnenschein and M. Zamaklar, *Phys. Rev. D* **74**, 106008 (2006) [arXiv:hep-th/0606195]; K. Hashimoto, T. Hirayama and A. Miwa, *JHEP* **0706**, 020 (2007) [arXiv:hep-th/0703024].
- [4] K. Nawa, H. Suganuma and T. Kojo, *Phys. Rev. D* **75**, 086003 (2007) [arXiv:hep-th/0612187]; *Prog. Theor. Phys. Suppl.* **168**, 231 (2007) [arXiv:hep-th/0701007]; D. K. Hong, M. Rho, H. U. Yee and P. Yi, *Phys. Rev. D* **76**, 061901 (2007) [arXiv:hep-th/0701276]; H. Hata, T. Sakai, S. Sugimoto and S. Yamato, arXiv:hep-th/0701280; D. K. Hong, M. Rho, H. U. Yee and P. Yi, *JHEP* **0709**, 063 (2007) [arXiv:0705.2632 [hep-th]].
- [5] O. Bergman and G. Lifschytz, *JHEP* **0704**, 043 (2007) [arXiv:hep-th/0612289];
- [6] O. Aharony, J. Sonnenschein and S. Yankielowicz, *Annals Phys.* **322**, 1420 (2007) [arXiv:hep-th/0604161].
- [7] A. Parnachev and D. A. Sahakyan, *Phys. Rev. Lett.* **97**, 111601 (2006) [arXiv:hep-th/0604173].
- [8] O. Bergman, G. Lifschytz and M. Lippert, *JHEP* **0711**, 056 (2007) [arXiv:0708.0326 [hep-th]].
- [9] N. Horigome and Y. Tanii, *JHEP* **0701**, 072 (2007) [arXiv:hep-th/0608198]; J. L. Davis, M. Gutperle, P. Kraus and I. Sachs, *JHEP* **0710**, 049 (2007) [arXiv:0708.0589 [hep-th]]; M. Rozali, H. H. Shieh, M. Van Raamsdonk and J. Wu, *JHEP* **0801**, 053 (2008) [arXiv:0708.1322 [hep-th]].
- [10] A. Parnachev, arXiv:0708.3170 [hep-th]; O. Aharony, K. Peeters, J. Sonnenschein and M. Zamaklar, arXiv:0709.3948 [hep-th].
- [11] R. Casero, E. Kiritsis and A. Paredes, *Nucl. Phys. B* **787**, 98 (2007) [arXiv:hep-th/0702155]; O. Bergman, S. Seki and J. Sonnenschein, *JHEP* **0712**, 037 (2007) [arXiv:0708.2839 [hep-th]]; A. Dhar and P. Nag, *JHEP* **0801**, 055 (2008) [arXiv:0708.3233 [hep-th]].
- [12] A. Karch and A. O'Bannon, *JHEP* **0709**, 024 (2007) [arXiv:0705.3870 [hep-th]]; A. O'Bannon, *Phys. Rev. D* **76**, 086007 (2007) [arXiv:0708.1994 [hep-th]].
- [13] V. G. Filev, arXiv:0706.3811 [hep-th]; T. Albash, V. G. Filev, C. V. Johnson and A. Kundu, arXiv:0709.1547 [hep-th]; T. Albash, V. G. Filev, C. V. Johnson and A. Kundu, arXiv:0709.1554 [hep-th].
- [14] J. Erdmenger, R. Meyer and J. P. Shock, *JHEP* **0712**, 091 (2007) [arXiv:0709.1551 [hep-th]].
- [15] E. Antonyan, J. A. Harvey, S. Jensen and D. Kutasov, arXiv:hep-th/0604017.
- [16] S. Caron-Huot, P. Kovtun, G. D. Moore, A. Starinets and L. G. Yaffe, *JHEP* **0612**, 015 (2006) [arXiv:hep-th/0607237].
- [17] D. T. Son and A. O. Starinets, *JHEP* **0209**, 042 (2002) [arXiv:hep-th/0205051].
- [18] A. Parnachev and D. A. Sahakyan, *Nucl. Phys. B* **768**, 177 (2007) [arXiv:hep-th/0610247].